Scientia Iranica A (2019) 26(4), 2299–2309

Sharif University of Technology
Scientia Iranica
Transactions A: Civil Engineering
http://scientiairanica.sharif.edu

Invited Paper

Effect of utilizing glass fiber-reinforced polymer on flexural strengthening of RC arches

H. Moradi[a], A.R. Khaloo[b,*], M. Shekarchi[b], and A. Kazemian[b]

a. *Department of Civil Engineering, School of Science and Engineering, Sharif University of Technology, International Campus, Kish Island, Iran.*
b. *Department of Civil Engineering, Sharif University of Technology, Tehran, Iran.*

Received 22 April 2019; received in revised form 15 July 2019; accepted 21 July 2019

KEYWORDS
Reinforced concrete arch;
Glass fiber-reinforced polymer;
Flexural strengthening;
Five-hinge mechanism;
Statistical analysis.

Abstract. An experimental study of the flexural behavior of Reinforced-Concrete (RC) arches strengthened with Glass Fiber-Reinforced Polymer (GFRP) layers was performed. A total of 36 specimens including 3 un-strengthened (control) and 33 strengthened RC arches were tested under centrally concentrated point load. The variables of this study were steel reinforcement ratio, number of GFRP layers, and location and arrangement of GFRP layers. Failure mode, load-displacement response of specimens, crack propagation patterns, and GFRP debonding were examined. The extrados strengthening method was shown to be more effective than the intrados strengthening one in improving the failure load and rigidity of the arches. However, applying excessive GFRP layers to the extrados could change the failure mode of arches from flexural to shear. The dominant failure mode of specimens was flexural and ductile due to the formation of five-hinge mechanism. Generally, GFRP strengthening could enhance the ultimate load carrying capacity, secant stiffness, and energy absorption capacity of arch specimens by up to about 154, 300, and 93 percent, respectively. Statistical analyses were performed to assess the level of influence of each considered parameter on the behavior of RC arches. Finally, analytical approach satisfactorily predicted the experimental data for arches with five-hinge failure mechanism.

1. Introduction

One type of structure that has received much attention throughout history is arch structures such as culverts, tunnels, bridges, domes, and underground municipal arch-shaped structures. Some major reasons for the popularity of this type of structures can be enumerated. First, they can be used in large-span bridges with no need for columns; second, they have high load-carrying capacity; and finally, they are architecturally attractive. Masonry materials were used in order to implement arch structures in the past [1,2]. Nowadays, these structural members are mainly constructed from RC materials. Some of the arch structures require to be rehabilitated and strengthened due to several reasons such as exposure to harsh environment, bad maintenance, and changes in design codes. Assorted methods and materials are applied for strengthening of arch structures. Using advanced Fiber Reinforced Polymer (FRP) materials is becoming popular in this respect. In fact, FRPs have excellent mechanical properties, corrosion resistance, and strength-to-weight ratio [3-5]. Also, FRP sheets are flexible and can easily be applied to the surfaces of arch-shaped structures.

The influence of using FRP materials on strength-

*. *Corresponding author. Tel.: +98 21 66164211*
E-mail address: khaloo@sharif.edu (A.R. Khaloo)

doi: 10.24200/sci.2019.21512

ening of typical structural members such as beams, columns, and walls with different materials of concrete and masonry has been investigated in the previous studies [6-11]. Moreover, the effectiveness of attaching FRP layers to the surfaces of masonry structural arch elements has been evaluated by some researchers [12,13]. However, a decisive conclusion has not been drawn about whether the extrados or intrados strengthening is more effective. On the one hand, some researchers concluded that intrados bonding was much more effective [14,15]; on the other hand, others proved that extrados strengthening had a better performance as it enabled the structure to show better response in terms of cohesion [13]. Also, it has been pointed out that the FRP layers in extrados strengthening have a greater contribution to holding of the bricks of masonry arches when loaded [16]. Bati and Rovero [14] experimentally assessed the behavior of masonry arches strengthened with CFRP strips. They showed that extrados reinforced arches had higher stiffness and ductility values than those with CFRP layers bonded to the intrados of the arch member. Extrados or intrados reinforcing can affect the failure mode of specimens. Oliveira et al. [15] revealed that masonry arches with GFRP strips at intrados experienced debonding of fibers from arch substrate and specimens with GFRP at extrados failed because of sliding along a mortar joint near the right supports. Foraboschi [17] showed that the width and spacing of FRP strips had considerable effect on the overall behavior of retrofitted masonry arches as well as the position of FRP composites. Valluzi and Modena [16] investigated the responses of some full-scale strengthened vaults loaded at one-fourth of their span. They concluded that GFRP strips were better than CFRP layers for rehabilitation of masonry arches since the Young's modulus of GFRPs was closer to masonry materials than that of CFRPs. Also, some researchers conducted numerical and analytical studies in order to predict the performance of retrofitted arches [18-20].

In recent years, researchers have focused on RC arches to investigate the influence of FRP materials attached to the extrados and intrados surfaces of these members. Hamed et al. [21] and Zhang et al. [22] performed experimental and analytical studies on externally bonded CFRP strengthened RC arches. The specimens were loaded unsymmetrically and CFRP composites were mounted on the extrados surface of shoulder and intrados surface of vault, which experienced the maximum tensile stress during the test. Various strengthening methods such as bonding and bonding-wrapping were compared in their study. It was concluded that the bonding-wrapping method was able to improve the load-bearing capacity and stiffness of arches better than the bonding method. Considerable research studies have been conducted on the masonry arches strengthened by GFRP layers. Nevertheless, no research has been reported on RC arches strengthened by GFRP in various arrangements.

In this experimental study, the influence of number of GFRP layers, location of GFRP composites, and steel reinforcement ratio (ρ) on the performance of RC arches is investigated by testing 36 specimens.

2. Materials

All of the specimens were casted with high-slump concrete and the same mixture design was considered for them. Using high-slump concrete was due to the curved shape of specimens. The specified compressive strength of concrete was 40 MPa. The ratio of gravel to sand was less than one and in order to achieve the suitable slump, Super-Plasticizer (SP) was added to the mixture. The amount of the added SP was 0.5 percent of the cement weight. The weight ratio of water to cement was 0.42. The maximum size of coarse aggregates was 8 mm and the fineness modulus of fine aggregate was 3.4.

To obtain the mechanical properties of steel rebars and GFRP layers, tensile tests were conducted based on ASTM A370-17 [23] and ACI 440.3R-04 [24], respectively. In order to attach the GFRP layers to the surface of RC arches, a high-strength epoxy adhesive was used the mechanical properties of which are given in Table 1 based on the catalog of the manufacturer.

3. Experimental program

3.1. Preparation of specimens

A total of 36 arch RC specimens were fabricated and tested in this experimental study. Span length, width, and thickness of all specimens were 1100 mm, 300 mm, and 100 mm, respectively. The radius of arch specimens was 607.1 mm, which means that the arches were a 130-degree slice of a complete circle. Also, the height of vault was 350 mm. A cover of 10 mm was considered for the specimens. Unidirectional GFRP layers with the thickness of 0.15 mm were used to strengthen the concrete arches. The diameter of longitudinal steel rebars and stirrups was 8 mm. The space between the stirrups was 25 mm along the span. In fact, to preclude the specimens from experiencing shear failure during the tests, shear design was developed and the transverse rebars were located close to each other. Figure 1 presents the geometry of RC arches. In order to prepare the curved steel bars, first, their radius and curvature were calculated. Then, the straight steel bars were turned into hoops with the specified radius using a machine, as shown in Figure 2(a). Thereafter, the curved rebars were cut with appropriate length (see Figure 2(b)). After that, a 180-degree hook with the

Table 1. Mechanical properties of materials.

Material	Young's modulus (GPa)	Yield stress (MPa)	Ultimate stress (MPa)	Compressive strength (MPa)	Ultimate strain (%)
Resin	3.5	—	30	100	1.0
Concrete	28.5	—	—	40	0.31
Steel	203	344	512	—	21
GFRP	76	—	2100	—	2.5

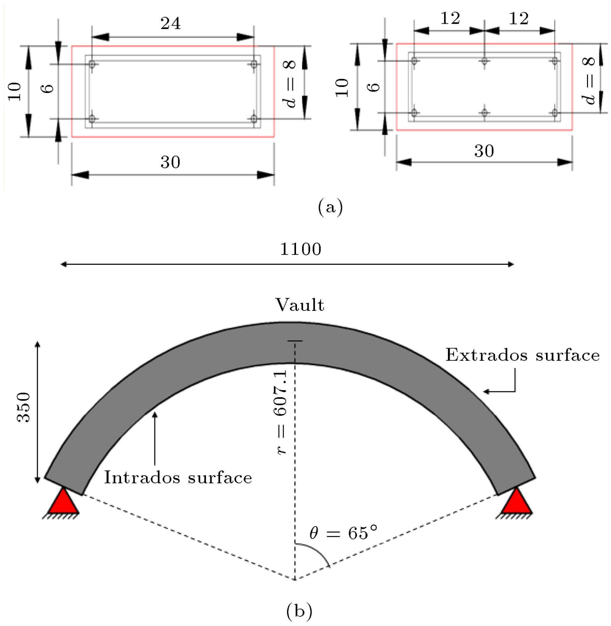

Figure 1. Geometry of specimens: (a) Cross section and reinforcement of RC arches and (b) arch dimensions (in mm).

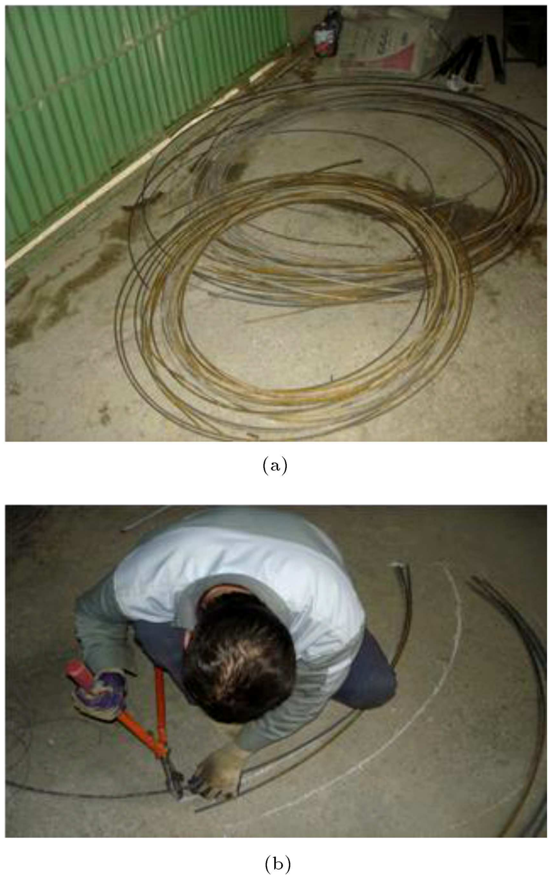

Figure 2. (a) Rebar hoops. (b) Cutting rebars with proper length.

length of 50 mm was created at both ends of steel bars making better bond between concrete and rebars.

Using steel plates with the thickness of 2 mm, the molds with proper curvature were constructed. In order to have a smooth surface at the top and bottom of the specimens and to make the casting process easy, concrete was casted through the lateral sides of the specimens as shown in Figure 3. Providing a smooth surface was indispensable for implementing GFRP layers. The arch specimens were removed from their molds 24 hours after casting and cured under wet burlap.

The external and internal surfaces of arches were grinded with fine sandpaper and cleaned with acetone in order to remove any particles and oil that could have detrimental effects on the bond between GFRP layers and RC arches. Two components of the epoxy adhesive (resin and hardener) were mixed with a proper ratio and applied to the extrados and intrados of specimens. Then, the GFRP layers were mounted on the adhesive layer and pressed to remove the air bobbles in the adhesive. The specimens were placed in a room with an environment of 21±2°C temperature and 65±5 percent relative humidity for 10 days for curing of epoxy. Since the GFRP layers would experience considerable stress concentration at both ends [25], the ends of strengthened specimens were wrapped by GFRP strips in order to prevent the GFRP layers from premature debonding during the tests (see Figure 4).

In order to make the test outcomes more reliable, 3 repetitions were tested for each strengthening method. Table 2 presents the designation and various strengthening configurations of each specimen. The specimens are labeled as Sx-yEzI-r, where x, y, z, and r represent the number of longitudinal steel rebars, number of GFRP layers attached to the extrados of

Table 2. Experimental program.

Specimen no.	Specimen designation	ρ (%)	Configuration and number of GFRP layers
1-3	S4-0E0I-(1∼3)	0.33	—
4-6	S4-0E1I-(1∼3)	0.33	Only one on intrados
7-9	S4-1E0I-(1∼3)	0.33	Only one on extrados
10-12	S4-1E1I-(1∼3)	0.33	One on extrados, one on intrados
13-15	S4-1E2I-(1∼3)	0.33	One on extrados, two on intrados
16-18	S4-2E1I-(1∼3)	0.33	Two on extrados, one on intrados
19-21	S6-0E0I-(1∼3)	0.5	—
22-24	S6-0E1I-(1∼3)	0.5	Only one on intrados
25-27	S6-1E0I-(1∼3)	0.5	Only one on extrados
28-30	S6-1E1I-(1∼3)	0.5	One on extrados, one on intrados
31-33	S6-1E2I-(1∼3)	0.5	One on extrados, two on intrados
34-36	S6-2E1I-(1∼3)	0.5	Two on extrados, one on intrados

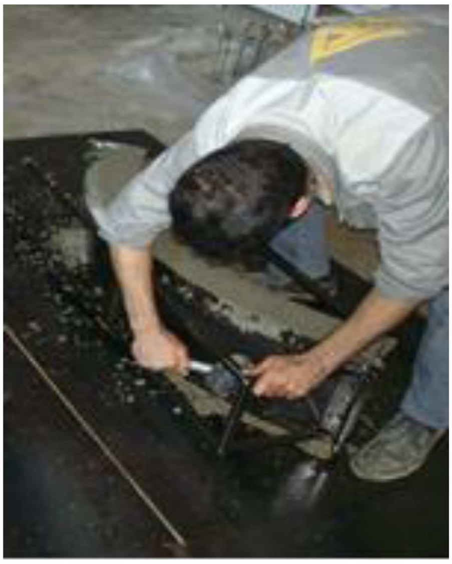

Figure 3. Casting process of concrete through lateral sides of specimens.

arch, number of GFRP layers attached to the intrados of arch, and number of repetitions, respectively. For instance, S6-2E1I-2 is the second repetition for the RC arches with 6 longitudinal steel bars, 2 GFRP layers mounted on extrados, and one GFRP layer attached to intrados.

3.2. Test set-up

Figure 5 depicts the test set-up used in the experiments. The arch specimens were placed over 2 simple supports (pinned supports) and then, loaded monotonically by a hydraulic jack with a capacity of 1000 kN. The actuator applied the load at mid-span to the extrados of vaults. The experiments were conducted under displacement control loading with a constant speed of 0.05 mm/sec. In order to transmit the load from the hydraulic jack to RC arches, a 300-mm long steel rod (similar to arch width) with the diameter of 20 mm was used. The load and displacement at mid-span of RC arches were recorded throughout the loading.

(a)

(b)

Figure 4. (a) A set of RC arches. (b) GFRP wrapping at both ends of arches.

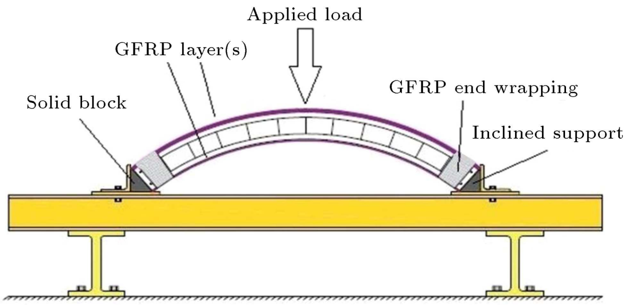

Figure 5. Test set-up.

4. Experimental results and discussion

4.1. Failure mode

Based on observations and outcomes of the test, 2 different failure modes occurred in experiments:

1. Flexural failure mode;
2. Shear failure mode.

Most of the control and strengthened RC arches experienced flexural failure, which was emanated by the formation of five-hinge mechanism [22]. Moreover, the strengthened specimens with 2 GFRP layers covering the extradoses of arches (S4-2E1I and S6-2E1I) collapsed because of shear failure at vault. The specimens experiencing shear failure mode were capable of carrying the maximum load in comparison with the other arches.

The specimens that failed due to the formation of five-hinge mechanism experienced some flexural cracks at intrados of the vault. Then, GFRP deboning at vault happened and the width and number of cracks increased. As the mid-span displacement increased, the GFRP debonding progressed and moved toward the supports. Thereafter, the flexural cracks were developed at shoulders of RC arches. Finally, the specimen failed because of the formation of the fourth and fifth hinges at shoulders as shown in Figure 6. The failure of these specimens was ductile, which is desirable in practice. No extrados debonding was observed during the tests.

In specimens failing under shear mode, some cracks formed at intrados and GFRP debonding at the intrados of vault occurred, like in other specimens. Then, a shear crack suddenly developed with a slope of almost 45 degrees and the RC arch collapsed before the formation of plastic hinge at vault, as can be seen in Figure 7. There were no noticeable cracks at the shoulders of arch. Also, extrados debonding did not happen in these specimens. The arches with the shear failure mode showed the highest ultimate load carrying capacity among the tested specimens, even though they did not reach their maximum flexural capacity. Their collapse was completely abrupt and brittle with a very loud sound.

(a)

(b)

Figure 6. (a) Flexural cracks and GFRP debonding at intrados of vault. (b) Formation of plastic hinge at shoulder.

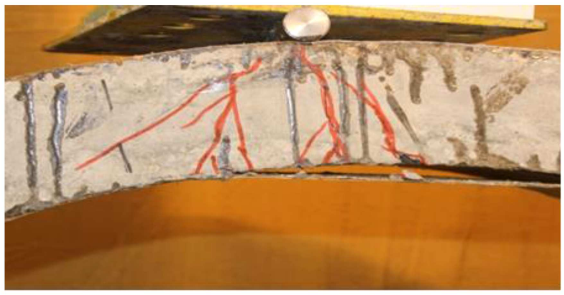

(a)

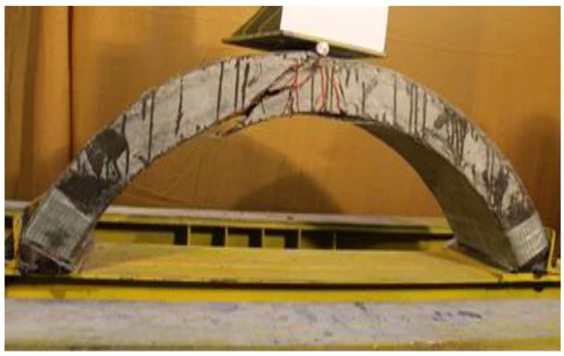

(b)

Figure 7. (a) Flexural cracks and GFRP debonding at intrados of vault. (b) Shear crack at vault.

4.2. Load-displacement behavior

Figure 8 depicts the typical load versus displacement diagram. Table 3 presents the test results in terms of the mean value of peak load, secant stiffness, energy

Table 3. Mean values of test results.

Specimen ID	Failure mode	Peak load (kN)	Peak load increase (%)	Secant stiffness (kN/mm)	Secant stiffness increase (%)	Energy absorption capacity (kN.mm)	Energy absorption capacity increase (%)	Deflection at Peak load (mm)
S4-0E0I	5-hinge	153.91	—	7.60	—	3168.20	—	33.54
S4-0E1I	5-hinge	179.33	16.52	8.98	18.16	3458.34	9.16	30.48
S4-1E0I	5-hinge	290.61	88.82	16.46	116.58	5480.61	72.99	25.91
S4-1E1I	5-hinge	320.68	108.36	21.72	185.79	5745.48	81.35	24.8
S4-1E2I	5-hinge	342.12	122.29	25.12	230.53	6040.82	90.67	22.31
S4-2E1I	Shear	391.87	154.61	30.43	300.39	2802.44	−11.55	15.66
S6-0E0I	5-hinge	183.25	—	9.67	—	2523.08	—	24.72
S6-0E1I	5-hinge	205.42	12.10	11.75	21.5	2885.26	14.35	21.21
S6-1E0I	5-hinge	311.83	70.17	20.59	112.93	4213.74	67.01	18.97
S6-1E1I	5-hinge	347.52	89.64	24.37	152.02	4546.81	80.21	18.02
S6-1E2I	5-hinge	367.92	100.77	27.81	187.59	4891.32	93.86	15.38
S6-2E1I	Shear	396.79	116.53	32.36	234.64	2197.98	−12.89	12.17

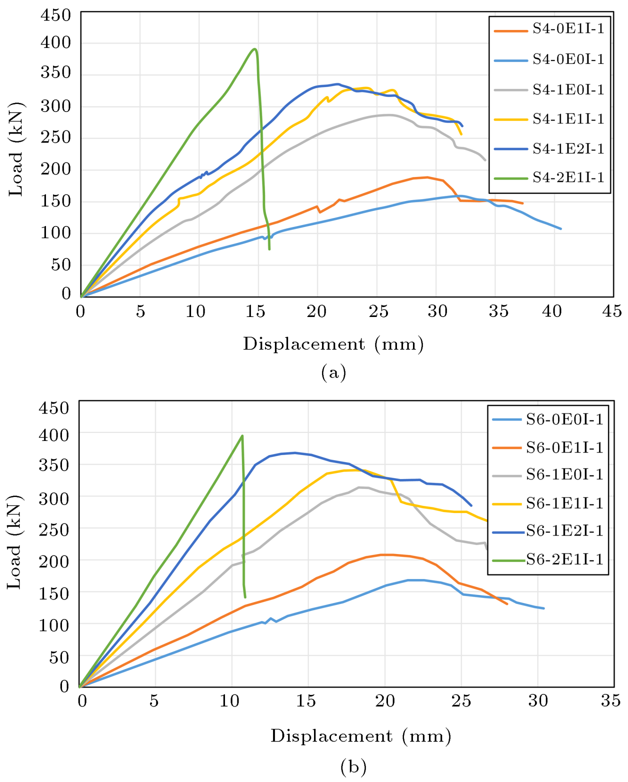

Figure 8. Load versus displacement diagram of (a) S4 specimens and (b) S6 specimens.

absorption capacity, and failure mode of control and strengthened arches.

Based on the test results, the effect of the presence of GFRP layers covering the intrados of arches on the ultimate load bearing capacity of specimens was not considerable in comparison with the influence of GFRP layers attached to the extrados of arches. The mean peak load of specimens strengthened with one layer of GFRP at intrados was 16.52 percent more than that in control specimens, whereas the ultimate load of the arch strengthened with one GFRP layer at extrados was improved by 88.82 percent. This can be attributed to 2 reasons. First, the debonding of GFRP at intrados of specimens could significantly diminish the contribution of GFRP layers in carrying the applied load. Second, the failure of arch was controlled by extrados surfaces of specimens since the fourth and fifth hinges were formed there and there was no GFRP debonding at external surface of arch. Moreover, the GFRP layers mainly worked in tension, and the extrados of shoulders and intrados of vault experienced tensile stress in compliance with the flexural moment diagram of specimens. Therefore, the ultimate load carrying capacity of RC arches could be improved significantly by applying the GFRP layers at extrados of shoulders.

Furthermore, since the strength of GFRP layers in compression was considerably low, there was scant difference between the failure loads of arches strengthened with the same number of GFRP layers at extrados and different numbers of GFRP layers at intrados. For instance, the mean failure loads of specimens S4-1E1I and S4-2E1I were 10.35 and 17.72 percent more than that of specimen S4-1E0I, respectively. These slight differences were due to the fact that as the number of GFRP layers applied to the intrados increased, the ultimate load bearing capacity of specimens improved [22].

In RC arches with low reinforcement (S4 specimens), applying the GFRP layers could improve the ultimate failure load more than in specimens with higher numbers of steel rebars (S6 specimens). The average ultimate load carrying capacity improvement for S4 arches was 98.12 percent, while the average increase in failure load for S6 arches was 77.84 percent.

4.3. Secant stiffness

The value of secant stiffness of each specimen (K_s) is calculated by using the load-displacement diagram of arches and defined by the following equation:

$$K_s = \frac{0.4P_u}{W_{0.4P_u}}, \tag{1}$$

where P_u and $W_{0.4P_u}$ are the ultimate load bearing capacity of specimen and mid-span displacement corresponding to 40 percent of failure load, respectively. As shown in Table 3, the extrados strengthening method could make the RC arches stiffer than intrados strengthening method did. Based on the test outcomes, the mean secant stiffness of specimens could be enhanced by up to 300 percent by attaching GFRP layers to the extrados surfaces of arches. On the contrary, the intrados strengthening method was not able to increase the secant stiffness of specimens significantly.

4.4. Energy absorption capacity

The capacity of RC arches to dissipate (absorb) energy can be calculated by the enclosed area under load-displacement diagram (at mid-span) of specimen. In other words, it can be defined by the following equation:

$$\text{Energy absorbtion capacity} = \int_{0}^{W_{0.9P_u}} P dw, \tag{2}$$

where P is the value of the applied load and $w_{0.9P_u}$ is the mid-span displacement corresponding to 90 percent of the ultimate load carrying capacity of specimens in the descending branch of the diagrams.

Table 3 presents the energy absorption capacity of control and strengthened specimens. It can be concluded that the mean energy absorption of control RC arches with 4 and 6 longitudinal steel bars is improved by 72.99 and 67.01 percent when a GFRP layer is applied to the extrados surface of specimens. It should be noted that specimens retrofitted with 2 GFRP layers at extrados of arch gave lower amounts of dissipated energy than control specimens. Although extrados strengthening method could improve the ultimate load carrying capacity of arches, it reduced the mid-span displacement corresponding to the peak load. In fact, as the number of GFRP layers attached to the extrados surface of specimens increases, the overall behavior of specimens changes from flexural failure to shear failure, which can considerably diminish the energy absorption capacity of arches. Hence, excessive use of GFRP layers on the extrados of arches could have some undesirable effects.

5. Statistical analysis

5.1. Normal distribution curves

In order to evaluate the consistency of the test results, the ultimate load carrying capacity of specimens was selected and the normal distribution curve was plotted based on 3 data points obtained for each group. Figure 9 indicates the probability density versus peak load for specimens. As can be seen in Figure 9, maximum variance is for control specimens. This is due to the fact that even slight variations in concrete at the shoulder of arch in tested specimens, such as local non-uniformities, can greatly affect the failure load of specimens. On the contrary, as the number of GFRP layers attached to the extradoses of arches increases, the non-uniformity of test results decreases between the specimens with similar geometries and strengthening arrangements. Generally, not only do the GFRP layers improve the response of RC arches, but also they make the behavior of specimens more predictable and consistent.

5.2. ANOVA analysis

An analysis of variance (ANOVA) was performed to assess the level of influence of the considered variables on the ultimate load bearing capacity of the RC arches

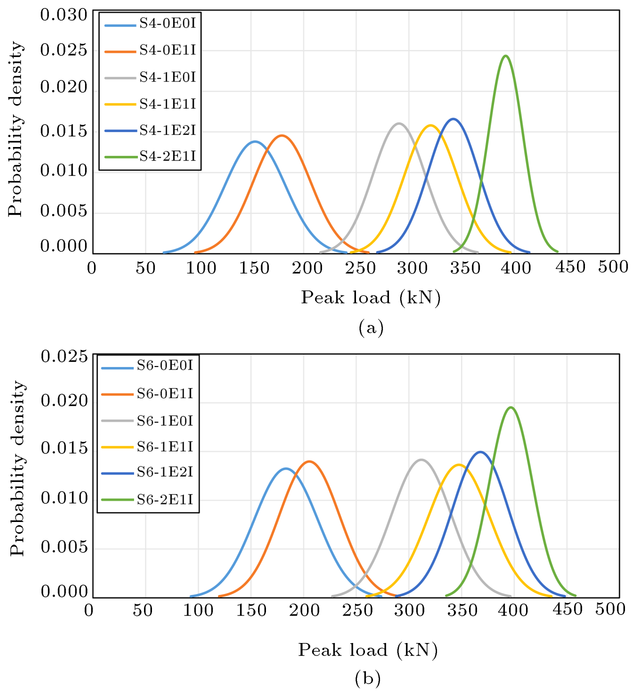

Figure 9. Normal distribution of (a) S4 specimens and (b) S6 specimens.

Table 4. Summary of ANOVA.

Factor	p-value
Factor 1, number of GFRP layers applied to the extrados	< 0.001
Factor 2, number of GFRP layers applied to the intrados	0.002
Factor 3, number of longitudinal steel bars	0.03
Interaction between factor 1 and factor 2	> 0.05
Interaction between factor 2 and factor 3	> 0.05
Interaction between factor 1 and factor 3	> 0.05
Interaction between all factors	> 0.05

and their potential interactions. ANOVA comprises collecting statistical models and their associated estimation procedures (such as the "variation" among and between groups) to analyze the differences among group means in a sample. In the present ANOVA, the first parameter considered was the number of longitudinal steel bars at 2 different levels (4 and 6 steel bars). The second variable was the number of GFRP layers applied to the extradoses of arches at 3 levels (0, 1, and 2 layers). The third parameter was the number of GFRP layers attached to the intradoses of specimens at 3 levels (0, 1, and 2 layers). ANOVA evaluates whether or not the differences between the recorded test results are statistically significant [26]. The p-value in Table 4 stands for the significance of test variable, which is compared with the significance level of α. Based on the common science and engineering practices, the significance level of α is equal to 0.05 [26]. If the p-value is equal to or less than the significance level, the considered parameter will be statistically significant.

Table 4 reveals the outcomes of ANOVA. The results prove that all of the 3 considered variables have significant statistical influence on the ultimate load carrying capacity of arches. However, the level of significance is higher for the number of GFRP layers applied to the extrados than for the other 2 variables. Moreover, the interactions between these parameters are not statistically significant since their p-values are more than 0.05.

6. Analytical study

The RC arches with simple supports have one degree of indeterminacy. Hence, they do not experience failure after formation of the first hinge at mid-span. In fact, after the formation of the first hinge, other hinges should be formed at the shoulders for failure of pinned-end arches, called five-hinge mechanism. This mechanism helps RC arches collapse at higher loads than straight beams do. Numerical prediction of the behavior of RC arches with the five-hinge failure mechanism requires several assumptions such as behavior of specific materials, bonding of FRP with the concrete, and changes in the type of load in extreme arch fibers (tension to compression and vice versa) in the 3 middle hinges. Nevertheless, analytical approaches are desirable for practical strengthening design of RC arches using FRP layers. Even though analytical predictions are simpler and faster in obtaining the capacity of strengthened arches, they usually give a good estimation of the behavior of arch response by utilizing the basic theory.

In order to calculate the internal forces and flexural strength of tested arches, the following assumptions are made:

- FRP has linear behavior in tension;
- Compressive strength of FRP layers is neglected;
- Steel rebars have elastic perfectly plastic behavior;
- Tensile strength of concrete is neglected;
- Strain distribution is linear.

The depth of neutral axis can be determined by the following formula, using trial-and-error procedure:

$$C = \frac{A_s f_s + A_f f_f - A'_s f'_s}{0.85 b f'_c}, \tag{3}$$

where A_s, A_f, and A'_s are the area of tension reinforcements, area of FRP applied to the tension surface of arch, and compression reinforcement, respectively. Also, f_s, f_f, f'_s, and f'_c denote the stress of tension reinforcements, the stress of FRP reinforcements mounted on the tension side, the stress of compression reinforcements, and compressive strength of concrete. b is width of the cross section.

The ultimate moment capacity of arches has been proposed analytically by Zhang et al. [22] as follows:

$$M_n = f'_c b z \left(h - \frac{z}{2}\right), \tag{4}$$

$$z = \frac{\rho_s f_a h + \eta \rho_f f_f h}{f'_c}, \tag{5}$$

where h and ρ_f are the height of cross section and FRP ratio. Also, η denotes the ratio of FRP stress

Table 5. Comparison between experimental and analytical calculations.

Specimen ID	Ultimate load, experimental results (kN)	Ultimate load, analytical results (kN)	Difference (%)
S4-0E0I	153.91	146.37	−5.2
S4-0E1I	179.33	158.10	−13.4
S4-1E0I	290.61	356.56	18.4
S4-1E1I	320.68	363.22	11.7
S4-1E2I	342.12	393.38	13.0
S4-2E1I	391.87	—	—
S6-0E0I	183.25	210.14	12.8
S6-0E1I	205.42	214.88	4.4
S6-1E0I	311.83	408.86	23.7
S6-1E1I	347.52	419.77	17.2
S6-1E2I	367.92	424.39	13.3
S6-2E1I	396.79	—	—

at collapse to its tensile strength.

$$f_a = \sqrt{f_y f_u}, \tag{6}$$

$$f_f = \varepsilon_{fe} E_f \leq f_{fu}, \tag{7}$$

where f_y, f_u, ε_{fe}, E_f, and f_{fu} are the yield strength of steel rebars, ultimate strength of steel rebars, strain of FRP layer mounted on the tension surface of the arch, Young's modulus of FRP, and tensile strength of FRP.

Table 5 presents and compares the flexural strengths of specimens obtained analytically and by experiments. As shown in Table 5, the test results have good agreement with analytical predictions.

7. Conclusions

This study examined the behavior of RC arches retrofitted by GFRP layers. The test variables were the number of longitudinal steel rebars, the number of GFRP layers, and the location of implemented GFRP layers. The experimental results were recorded and presented in terms of ultimate load bearing capacity, secant stiffness, and energy absorption capacity. The following conclusions were drawn from experimental results and statistical analysis:

- The extrados strengthening approach was able to improve the failure load of RC arches more than intrados strengthening method was. However, excessive application of GFRP layers to the extrados surface of arches could change the failure mode from ductile and flexural to brittle and shear, which is not desirable in practice;
- Extrados strengthening was much more effective than intrados strengthening in improving the rigidity of RC arches. In fact, the secant stiffness of specimens could be enhanced by up to 300 percent by applying 2 layers of GFRP to the extrados in comparison with control arches. However, the rigidity of specimens rehabilitated by one layer of GFRP at intrados of arch did not improve considerably;
- As the amount of steel reinforcement ratio of RC arch decreased, the efficacy of GFRP strengthening increased and the GFRP layers were able to improve the behavior of specimens more than those with high steel reinforcement ratio;
- In the evaluation of normal distribution curves, it was observed that the behavior of RC arches became more consistent and predictable as they were strengthened by GFRP layer, particularly when the GFRP layers were applied to the extradoses of arches. This was due to the fact that the GFRP layers covered the critical moment regions of the structure and if there was any inconsistency, such as local non-uniformity, in concrete in these regions, the GFRP layers would cover them up and prevent stress concentration;
- The results of ANOVA analysis indicated that all of the 3 parameters considered in the experiments (number of steel rebars, GFRP layers at extrados, and GFRP layers at intrados) had statistically significant effect on the peak load of specimens. Moreover, the ANOVA analysis proved that the effect (significance level) of GFRPs applied to the extrados was more than that of the other 2 parameters;
- Analytical predictions presented herein had good correlation with the experimental results, which indicated the level of improvement in flexural capacity by FRP layers.

Acknowledgments

The authors are grateful to the staff and technicians of the strong floor laboratory for the supports they provided. Also, partial support of Iran National Science Foundation and the Center of Excellence in Structures and Earthquake Engineering was instrumental in conducting this research study.

References

1. Garmendia, L., San-José, J.T., García, D., et al. "Rehabilitation of masonry arches with compatible advanced composite material", *Construction and Building Materials*, **25**(12), pp. 4374-4385 (2011).
2. Alves, M., Vaz, C., Gomes, A., et al. "Restoration of the masonry arch bridge over Jamor river in the national palace of queluz", In *Structural Analysis of Historical Constructions*, R. Aguilar, Ed., RILEM Bookseries, Springer, Cham, **18**, pp. 2483-2491 (2019).
3. Theriault, M. and Benmokrane, B. "Effects of FRP reinforcement ratio and concrete strength on flexural behavior of concrete beams", *Journal of Composites for Construction*, **2**(1), pp. 7-16 (1998).
4. Tahsiri, H., Sedehi, O., Khaloo, A., et al. "Experimental study of RC jacketed and CFRP strengthened RC beams", *Construction and Building Materials*, **95**, pp. 476-485 (2015).
5. Grace, N.F., Soliman, A.K., Abdel-Sayed, G., et al. "Behavior and ductility of simple and continuous FRP reinforced beams", *Journal of Composites for Construction*, **2**(4), pp. 186-194 (1998).
6. Hosseinpour, M., Celikag, M., and Akbarzadehbengar, H. "Strengthening and shape modification of fire-damaged concrete with expansive cement concrete and CFRP wrap", *Scientia Iranica*, **26**(2), pp. 699-708 (2019).
7. Mostofinejad, M. and Noormohamadi, M. "Analysis of RC beams strengthened with FRP sheets under shear and flexure using MCFT", *Scientia Iranica*, **26**(2), pp. 634-640 (2019).
8. Hosseini, A., Khaloo, A.R., and Fadaee, S. "Seismic performance of high-strength concrete square columns confined with carbon fiber reinforced polymers (CFRPs)", *Canadian Journal of Civil Engineering*, **32**(3), pp. 569-578 (2005).
9. Khalou, A.R. and Esmaeeli, A. "Strengthening design limitations of an RC frames using FRP column wrapping considering column-to-beam strength ratio.", *Scientia Iranica*, **14**(5), pp. 405-413 (2007).
10. Carozzi, F.G., Colombi, P., Fava, G., et al. "Mechanical and bond properties of FRP anchor spikes in concrete and masonry blocks", *Composite Structures*, **183**, pp. 185-198 (2018).
11. Shadan, F., Khaloo, A., and Shadan, P. "Numerical study on flexural strengthening of squat RC shear wall using FRP laminates", *Scientia Iranica*, **22**(1), pp. 144-156 (2015).
12. Tao, Y., Stratford, T.J., and Chen, J.F. "Behaviour of a masonry arch bridge repaired using fibre-reinforced polymer composites", *Engineering Structures*, **33**(5), pp. 1594-1606 (2011).
13. Cancelliere, I., Imbimbo, M., and Sacco, E. "Experimental tests and numerical modeling of reinforced masonry arches", *Engineering Structures*, **32**(3), pp. 776-792 (2010).
14. Bati, S.B. and Rovero, L. "Towards a methodology for estimating strength and collapse mechanism in masonry arches strengthened with fibre reinforced polymer applied on external surfaces", *Materials and Structures*, **41**(7), pp. 1291-1306 (2008).
15. Oliveira, D.V., Basilio, I., and Lourenço, P.B. "Experimental behavior of FRP strengthened masonry arches", *Journal of Composites for Construction*, **14**(3), pp. 312-322 (2010).
16. Valluzzi, M.R. and Modena, C. "Experimental analysis and modelling of masonry vaults strengthened by FRP", In *Historical Constructions, Proc., 3rd Int. Seminar*, Guimarães, Portugal: University of Minho, pp. 627-636 (2001).
17. Foraboschi, P. "Strengthening of masonry arches with fiber-reinforced polymer strips", *Journal of Composites for Construction*, **8**(3), pp. 191-202 (2004).
18. De Lorenzis, L., Dimitri, R., and La Tegola, A. "Reduction of the lateral thrust of masonry arches and vaults with FRP composites", *Construction and Building Materials*, **21**(7), pp. 1415-1430 (2007).
19. Caporale, A., Feo, L., Hui, D., et al. "Debonding of FRP in multi-span masonry arch structures via limit analysis", *Composite Structures*, **108**, pp. 856-865 (2014).
20. Elmalich, D. and Rabinovitch, O. "Stress analysis of monolithic circular arches strengthened with composite materials", *Journal of Composites for Construction*, **13**(5), pp. 431-441 (2009).
21. Hamed, E., Chang, Z.T., and Rabinovitch, O. "Strengthening of reinforced concrete arches with externally bonded composite materials: Testing and analysis", *Journal of Composites for Construction*, **19**(1), p. 04014031 (2014).
22. Zhang, X., Wang, P., Jiang, M., et al. "CFRP strengthening reinforced concrete arches: Strengthening methods and experimental studies", *Composite Structures*, **131**, pp. 852-867 (2015).
23. ASTM A370-17, *Standard Test Methods and Definitions for Mechanical Testing of Steel Products*, American Society for Testing and Materials (ASTM) international, West Conshohocken, PA (2017).
24. ACI440 3R-04, *Guide Test Methods for Fiber-Reinforced Polymers (FRPs) for Reinforcing or Strengthening Concrete Structures*, Farmington Hills (USA), American Concrete Institute (2004).
25. Malek, A.M., Saadatmanesh, H., and Ehsani, M.R. "Prediction of failure load of R/C beams strengthened with FRP plate due to stress concentration at the plate end", *ACI Structural Journal*, **95**, pp. 142-152 (1998).

26. Montgomery, D.C. and Runger, G.C., *Applied Statistics and Probability for Engineers*, 7th Edn., John Wiley & Sons (2018).

Biographies

Hossein Moradi received his BSc degree in Civil Engineering from Islamic Azad University, Tehran, Iran, in 1995 and his MSc degree in Structural Engineering from Islamic Azad University, Science and Research Branch, Tehran, Iran, in 2010. He is currently a PhD candidate in Structural Engineering in the International Campus of Sharif University of Technology. His main research interests are related to experimental analysis of RC structures and seismic strengthening techniques.

Alireza Khaloo received his PhD degree in Structural Engineering in 1986 from North Carolina State University. He is currently Professor at Sharif University of Technology, Tehran, Iran. His research interests include topics related to structural engineering, RC structures, concrete composite materials, materials of construction, and earthquake engineering.

Mohammad Shekarchi received his BSc degree in Civil Engineering from Imam Khomeini International University, Qazvin, Iran, in 2014 and his MSc degree in Earthquake Engineering from Sharif University of Technology, Tehran, Iran, in 2017. He is currently working as a Research Assistant with Professor Alireza Khaloo. His main research interests are strengthening of structural members, FRP composites, construction materials, and mechanics of materials.

Alireza Kazemian received his BSc degree in Civil Engineering in 2014 and his MSc degree in Structural Engineering both from Sharif University of Technology, Tehran, Iran. He is currently a PhD candidate at University at Buffalo. His research interest is rehabilitation and retorting of structures as well as large-scale experimental testing.